

TRIB2004-64347

THE SLIDING AND ROLLING OF A CYLINDER AT THE NANO-SCALE

O. Taylan Sari, George G. Adams, Sinan Müftü
Department of Mechanical and Industrial Engineering
Northeastern University, Boston, MA 02115
Email: adams@neu.edu

ABSTRACT

The behavior of a nano-scale cylindrical body (e.g. a fiber), lying on a substrate and acted upon by a combination of normal and tangential forces, is the subject of this investigation. As the scale decreases to the nano level, adhesion becomes an important issue in this contact problem. Thus this investigation treats the two-dimensional plane strain elastic deformation of both the cylinder and the substrate during a rolling/sliding motion, including the effect of adhesion using the Maugis model. For the initiation of sliding, the Mindlin approach is used, whereas for rolling, the Carter approach is utilized. Each case is modified for nano-scale effects by including the effect of adhesion on the contact area and by using the adhesion theory of friction for the friction stress. Analytical results are given for the normal and tangential loading problems, including the initiation of sliding and rolling in terms of dimensionless quantities representing adhesion, cylinder size, and applied forces.

INTRODUCTION

Adhesion of cylindrical bodies on a substrate is encountered in nano-wires, carbon nano-tubes and nano-fibers, and in different fields such as microbiology, microelectronics, and MEMS/NEMS devices. Determination of the forces necessary to roll or slide a cylindrical body on the substrate are important quantities to know in these applications. In some cases it is important to manipulate these single fibers to form a structure whereas in other instances the sliding and rolling motions are important in contamination removal processes.

In this paper the adhesion of contacting cylinders, or equivalently a cylinder in contact with a half space, at the nano-scale is considered. If the cylinder is subjected to a combined tangential and normal loading it may remain at rest, roll, slide or undergo a complex motion depending on the magnitudes and the application points of the loading. The elastic behavior of the cylindrical body and half-space with adhesion are investigated using the plane strain theory of elasticity. A similar problem was treated in the thesis by Sari [1].

Numerous studies have been conducted on the adherence of spherical bodies. Bradley [2] found the pull-off force required to separate two rigid spherical bodies, of radii R_1 and R_2 , to be $F = 2\pi wR$ where $R = R_1R_2/(R_1 + R_2)$ is the equivalent radius of curvature, w is the work of adhesion $w = \gamma_1 + \gamma_2 - \gamma_{12}$, with the surface energies of the contacting bodies γ_1 and γ_2 , and the interface energy of the two surfaces γ_{12} .

Johnson, Kendall and Roberts (JKR) presented a theory on the adherence of deformable elastic bodies [3]. In the JKR approximation, the adhesion outside the contact region is assumed to be zero, and the contact area is larger than the Hertz contact area. The pull-off force was found to be $F = (3/2)\pi wR$.

Derjaguin, Muller and Toporov (DMT) presented another theory where the adhesion force is considered outside the contact area, but the form of the contact stress distribution is assumed to be unaffected [4]. The same pull-off force as the Bradley relation was found. It should be noted that F is independent of the elastic properties of the materials, for both JKR and DMT theories.

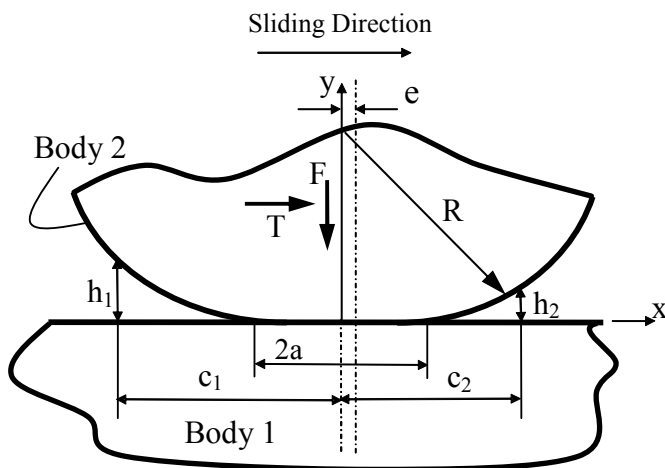


Figure 1. Contact of a cylinder with a half-space under normal and tangential loading.

Although the JKR and DMT theories seem to be competitive, Tabor [5] showed that these two theories represent the extremes of a parameter $\mu = (Rw^2 / E^2 z_0^2)^{1/3}$, where E is the composite Young's modulus and z_0 is the equilibrium spacing. Thus bodies in which the elastic deformation is large compared to the range of surface forces are in the JKR regime, whereas the DMT regime corresponds to elastic deformations which are much less than the range of surface forces. Greenwood constructed an adhesion map that covers these regimes [6].

Maugis presented a model for the transition between the JKR and DMT theories [7]. Similar to the Dugdale model of a crack, the Maugis model assumes a constant tensile surface stress σ_0 in regions where the surfaces are separated by a distance less than h , where the adhesion separation distance h is obtained from the relation $w = \sigma_0 h$. When this work of adhesion is set equal to that for the Lennard-Jones potential, h is found to be $0.97 z_0$, where σ_0 is taken as the theoretical strength. Baney and Hui [8] used the Maugis model to investigate the two-dimensional problem of the adhesion of two circular cylinders. Results are given for the contact and adhesion regions as functions of the applied normal force and also for the pull-off force.

The nano-scale sliding and rolling analysis treated in this paper differs from the corresponding macro-scale problem in two important ways. First, due to the small scale of the contact area, adhesion becomes important. The Maugis model is used to approximate the adhesive stress outside the contact region in a manner similar to Baney and Hui. Second, in the macro scale Coulomb friction, which states that frictional force is proportional to the normal load, is considered valid. At the nano-scale, however, where the contact radius is on the order of 10 nm or less, a single real contact area and constant shear stress are assumed for sliding.

THEORY AND DISCUSSION OF THE RESULTS

The contact of a cylindrical body of radius R with a flat surface is investigated. The results are equally valid for the contact of two cylinders by using the equivalent radius of curvature. Linear plane strain elasticity is used throughout, which implies that the forces are given per unit length.

According to plane strain linear elasticity [9], the derivative of the surface normal displacements can be written in terms of normal and shear stresses as,

$$\frac{d(u_y^{(1)} - u_y^{(2)})}{dx} = \frac{A}{4\pi} \int_{-c}^c \frac{p_y(\xi) d\xi}{x - \xi} - \frac{B}{4} p_x(x). \quad (1)$$

Similarly the relation between the derivative of the relative displacements of the bodies in the tangential direction and the boundary stresses is given by

$$\frac{d(u_x^{(1)} - u_x^{(2)})}{dx} = -\frac{A}{4\pi} \int_{-a}^a \frac{p_x(\xi) d\xi}{x - \xi} - \frac{B}{4} p_y(x) \quad (2)$$

In (1)-(2) p_x is the tangential traction in the x -direction and the contact pressure p_y is considered positive in compression. The material parameters A and B are given by

$$A = \frac{4(1-\nu_1)}{G_1} + \frac{4(1-\nu_2)}{G_2} = \frac{8}{E}, \quad B = \frac{2-4\nu_1}{G_1} - \frac{2-4\nu_2}{G_2},$$

$$\frac{1}{E} = \frac{1-\nu_1^2}{E_1} + \frac{1-\nu_2^2}{E_2}, \quad E_i = 2G_i(1+\nu_i) \quad (3)$$

where G_1, G_2 are the shear moduli, ν_1, ν_2 are the Poisson's ratios and E_1, E_2 are the moduli of elasticity of bodies "1" and "2" respectively, and E is the composite modulus. Equation (1) can be simplified for either identical materials ($B=0$) or for the frictionless case ($p_x(x)=0$). Even if the materials are not identical, the effect of the constant B is usually small [10] and is often neglected. Thus normal/shear stresses do not produce relative tangential/normal displacements.

Normal Loading

Consider normal loading in which a normal load F is applied to a cylinder with the tangential force T equal to zero. This problem has been solved by Baney and Hui [8], but their analysis is summarized here because the results of the normal loading problem determine the contact region used in the sliding and rolling analysis. There exists a central contact zone ($-a < x < a$) surrounded by two adhesion zones ($a < |x| < c$) in which the separated surfaces are under a constant tensile stress as described by the Maugis adhesion model [7]. This configuration is shown in Fig. 1 where, by symmetry, $c_1 = c_2 = c$, $h_1 = h_2 = h$, and $e = 0$. The tensile adhesive stress is effective up to a separation h , beyond which it vanishes.

The relation for the deformations in the normal direction at the contact interface is

$$u_y^{(1)} - u_y^{(2)} = -\delta_0 + \frac{x^2}{2R}, \quad -a < x < a \quad (4)$$

in the contact zone, where δ_0 is the maximum cylinder penetration which occurs at the center of the contact zone.

By proceeding as Baney and Hui [8], Eqs. (1) and (4) are combined using the Maugis condition in the adhesion zones

$$p_y(x) = -\sigma_0, \quad -c < x < -a, \quad a < x < c \quad (5)$$

with $B=0$. The solution is given by the superposition of the Hertz solution, the solution for an exterior crack [11], and the homogeneous solution of (1). That superposition of solutions is also subject to the conditions that the stress is bounded at both ends ($x = \pm a$). The result is [8],

$$p_y(x) = \frac{E}{2R} \sqrt{a^2 - x^2} - \frac{2\sigma_0}{\pi} \tan^{-1} \sqrt{\frac{c^2 - a^2}{a^2 - x^2}}, \quad -a < x < a \quad (6)$$

Because the contact half-width (a) and the adhesion half-width (c) are both unknown, two extra equations are necessary. These equations are obtained by using the force equilibrium in the y -direction, and by using the relation for the relative separation of the two bodies at $x=c$ and $x=a$. These give the following nondimensional equations,

$$\bar{F} = \bar{a}^2 - \lambda \bar{a} \sqrt{m^2 - 1}, \quad (7)$$

and

$$\frac{1}{2} \lambda \bar{a}^2 \left[m \sqrt{m^2 - 1} - \ln(m + \sqrt{m^2 - 1}) \right] + \frac{1}{2} \lambda^2 \bar{a} \left[\sqrt{m^2 - 1} \ln(m + \sqrt{m^2 - 1}) - m \ln(m) \right] = 1 \quad (8)$$

where the following nondimensional variables are used,

$$\bar{F} = \frac{F}{(\pi E w^2 R)^{1/3}}, \quad \bar{a} = \frac{a}{2(R^2 w / \pi E)^{1/3}}, \quad (9)$$

$$\lambda = \frac{4\sigma_0}{(\pi^2 E^2 w / R)^{1/3}}, \quad m = \frac{c}{a}$$

It is noted that Eqs. (7) and (8) form a pair of coupled nonlinear equations with \bar{F} known and \bar{a} and m unknown. These equations are solved numerically. The results for the dimensionless contact half-width (\bar{a}) vs. the dimensionless normal force (\bar{F}) for various values of λ are shown in Fig. 2. As discussed in [8], large λ correspond to the JKR regime, small λ approach Hertz contact, and when λ is of order unity the results can be approximated by the DMT theory. For nonzero λ there is a pull-off force which, for a sufficiently large value of λ , occurs at a nonzero contact radius.

Initiation of Sliding

Tangential forces can be transmitted by friction in contacting bodies. Consider a cylinder in contact with a half-space, compressed by a normal force F , and acted upon by a tangential force T (Fig. 1). With the normal load constant, the tangential force is gradually increased in order to initiate sliding. The problem is solved for the uncoupled case, i.e. $B=0$ in Eq. (1). Thus the contact area remains in a state of stick during the application of the normal load and the contact area remains constant during the application of the tangential force.

Mindlin studied the initiation of macro-scale sliding of a cylinder using Coulomb friction without adhesion and showed that slip will occur at the edges of the contact zone [12]. According to Mindlin's theory there exists a central stick zone ($|x| < d$) surrounded by slip zones symmetrically located in both the leading and trailing edges.

In nano-scale contacts, adhesion between the two bodies will affect the contact width. This effect in cylindrical contacts is described in the previous section. With respect to tangential loading, in the macro-scale Coulomb friction is used, whereas at the nano-scale the friction stress in the slip zone is assumed to be constant, as in the case of the adhesion theory of friction.

The relation between the relative tangential deformations of the bodies to the boundary stresses is given by Eq. (2). In the slip regions the following equation prevails,

$$p_x(x) = \tau_0, \quad d < |x| < a \quad (10)$$

where τ_0 is the shear strength. In the stick region, we have,

$$\frac{d(u_x^{(1)} - u_x^{(2)})}{dx} = 0, \quad -d < x < d \quad (11)$$

Prior to the initiation of global sliding motion, the horizontal shift (i.e. $u_x^{(1)} - u_x^{(2)}$) of the bodies in the stick zone ($-d < x < d$) will be constant.

The solution of Eq. (2) subject to (10)-(11) is found by superposition of the solution for an external crack loaded by a symmetric constant shear stress in a finite region near the crack tip [17, p. 110],

$$\tau_{xy} = -\frac{2\tau_0}{\pi} \left\{ \sqrt{\frac{a^2 - d^2}{d^2 - x^2}} - \tan^{-1} \sqrt{\frac{a^2 - d^2}{d^2 - x^2}} \right\}, \quad -d < x < d \quad (20)$$

and the homogeneous solution of Eq. (2) [19]

$$\tau_{xy} = \frac{D_0}{\sqrt{d^2 - x^2}}, \quad -d < x < d \quad (12)$$

where D_0 is determined from the condition that τ_{xy} is bounded at $x = |d|$. Thus the shear stress in the stick region becomes

$$\tau_{xy} = \frac{2\tau_0}{\pi} \tan^{-1} \sqrt{\frac{a^2 - d^2}{d^2 - x^2}}, \quad -d < x < d. \quad (13)$$

Force balance in the horizontal direction can be used to find the relation between the half-length of the stick zone (d) and the applied shear force (T). This procedure gives

$$T = 2(a-d)\tau_0 + \int_{-d}^d \tau(\xi) d\xi = 2\tau_0 \sqrt{a^2 - d^2}. \quad (14)$$

The integral in (14) has been evaluated in [8]. As the tangential force reaches the critical value of $2a\tau_0$, a state of complete slip (i.e. global sliding) occurs with $d = 0$.

Pure Sliding

If the contacting cylinder has a relative sliding motion with respect to the plane, there need not be symmetry due to the nonlinear nature of adhesion. In this case, the origin of the coordinate system will be chosen to be in the center of the contact region. The eccentricity e indicates the value of x corresponding to the apex of the undeformed cylinder. The leading adhesion zone will be a strip ($a < x < c_2$) and the trailing adhesion zone will be another strip ($-c_1 < x < -a$), as shown in Fig. 1.

The relation between the deformations of the bodies in the y -direction inside the contact is

$$u_y^{(1)} - u_y^{(2)} = -\delta_0 + \frac{(x-e)^2}{2R}. \quad (15)$$

The same elasticity formulation used for the symmetric normal contact can be used here i.e. Eq. (1) subject to (15) in the contact region $-a < x < a$. The solution can be found by the superposition of four problems. The first problem is the solution for a constant tensile stress in the leading edge ($a < x < c_2$) and the second is for a constant tensile stress in the trailing edge ($-c_1 < x < -a$). These solutions, which correspond to an external crack, are in Tada et al. [11, p. 107]. The Mode I stress intensity factors at the leading and trailing edges are

$$K_I(a) = -\sigma_0 \sqrt{\frac{a}{\pi}} \left\{ (1+m_2) \sqrt{m_2^2 - 1} + (1-m_1) \sqrt{m_1^2 - 1} \right\}$$

$$K_I(-a) = -\sigma_0 \sqrt{\frac{a}{\pi}} \left\{ (1+m_1) \sqrt{m_1^2 - 1} + (1-m_2) \sqrt{m_2^2 - 1} \right\} \quad (16)$$

where $m_1 = c_1/a$ and $m_2 = c_2/a$. The third problem corresponds to the solution of (1) and (15) without adhesion, i.e. a Hertz type solution with an eccentricity which can be found using [13]

$$p_Y(x) = \frac{E}{2R} \left(\sqrt{a^2 - x^2} - e \sqrt{\frac{a-x}{a+x}} \right), \quad -a < x < a \quad (17)$$

and the fourth is the homogeneous solution of (1), i.e.

$$p_Y(x) = D / \sqrt{a^2 - x^2}, \quad -a < x < a \quad (18)$$

The sum of these four solutions must be such that the normal stress is bounded at the ends at $x = |a|$. Recall that the Mode I stress intensity factor at $x = a$ is defined by

$$K_I(a) = \lim_{x \rightarrow a} \sqrt{2\pi(a-x)} \tau_{xy}, \quad (19)$$

The bounded normal stress condition at $x = a$ gives

$$D = -\frac{\sigma_0 a}{\pi} \left\{ (1+m_2) \sqrt{m_2^2-1} + (1-m_1) \sqrt{m_1^2-1} \right\}, \quad (20)$$

whereas the requirement that the normal stress must be bounded at $x = -a$, becomes

$$e = \frac{\sigma_0 R}{E\pi} \left\{ (1+m_1) \sqrt{m_1^2-1} + (1-m_2) \sqrt{m_2^2-1} \right\} + \frac{DR}{Ea} \quad (21)$$

When the cylinder is in a state of steady sliding, the adhesion effect in the trailing edge is assumed to be larger than in the leading edge. This assumption is considered valid because the surface will be partially cleaned due to the sliding motion of the contacting surfaces. This effect is accounted for by taking the adhesion separation distance in the trailing edge (h_1) larger than in the leading edge (h_2), whereas σ_0 is assumed unchanged. Due to the difference between h_1 and h_2 , the adhesion width values will not be the same in the leading and the trailing edges. Since there are two more unknowns, the separation equations must be written for both the leading and trailing edges. At the leading edge this procedure gives:

$$(u_y^{(1)} - u_y^{(2)})_{a^{c_2}} = \frac{(c_2 - e)^2 - (a - e)^2}{2R} - h_2 \quad (22)$$

and at the trailing edge it yields:

$$(u_y^{(1)} - u_y^{(2)})_{-a^{-c_1}} = \frac{(-c_1 - e)^2 - (-a - e)^2}{2R} - h_1 \quad (23)$$

Superposition of the four solutions yields

$$\begin{aligned} & \frac{2\sigma_0 a m_2}{\pi E h_1} (m_2^2 - 1) + \frac{2\sigma_0 a}{\pi E h_1} \left[(m_1 + m_2) \cosh^{-1} \left| \frac{1 + m_1 m_2}{m_1 + m_2} \right| \right. \\ & \left. - m_1 \sqrt{m_1^2 - 1} \sqrt{m_2^2 - 1} \right] - \frac{a^2}{2R h_1} \left[(m_2 - 2e/a) \sqrt{m_2^2 - 1} \right. \\ & \left. - (1 - 2e/a) \ln(m_2 + \sqrt{m_2^2 - 1}) \right] + \frac{2D}{E h_1} \ln(m_2 + \sqrt{m_2^2 - 1}) \\ & = -\frac{h_2}{h_1} \end{aligned} \quad (24)$$

from the leading edge condition and

$$\begin{aligned} & \frac{2\sigma_0 a m_1}{\pi E h_1} (m_1^2 - 1) + \frac{2\sigma_0 a}{\pi E h_1} \left[(m_1 + m_2) \cosh^{-1} \left| \frac{1 + m_1 m_2}{m_1 + m_2} \right| \right. \\ & \left. - m_2 \sqrt{m_1^2 - 1} \sqrt{m_2^2 - 1} \right] - \frac{a^2}{2R h_1} \left[(m_1 + 2e/a) \sqrt{m_1^2 - 1} \right. \\ & \left. - (1 - 2e/a) \ln(m_1 + \sqrt{m_1^2 - 1}) \right] + \frac{2D}{E h_1} \ln(m_1 + \sqrt{m_1^2 - 1}) \\ & = -1 \end{aligned} \quad (25)$$

for the trailing edge.

The applied normal force can be found from force equilibrium in the y -direction. Due to the asymmetry, a resultant moment will act on the upper body due to the asymmetric normal stress distribution. If moment equilibrium is written with respect to the center of contact, the resultant moment (clockwise direction acting on the half-space taken to be positive). The applied normal force and the resultant moment are given in nondimensional form by,

$$\bar{F} = \frac{\pi}{2} \lambda \bar{D} \bar{a} + \bar{a}^2 - 2\bar{e} \bar{a}^2, \quad \bar{M} = \bar{e} \bar{a}^3, \quad (26)$$

where the following nondimensional quantities are used,

$$\frac{2\sigma_0 a}{\pi E h_1} = \frac{\lambda^2 \bar{a}}{4}, \quad \frac{2D}{E h_1} = \frac{\pi \bar{D} \lambda^2 \bar{a}}{4}, \quad \bar{D} = \frac{D}{\sigma_0 a}, \quad (27)$$

$$\frac{a^2}{R h_1} = \lambda \bar{a}^2, \quad \bar{e} = \frac{e}{a}, \quad \bar{M} = \frac{M}{2wR}$$

in which $w = \sigma_0 h_1$. Thus Eqs. (24)-(25), along with the explicit expressions in (20)-(21), and the nondimensional quantities in (27), represent a pair of equations which, for specified λ and h_1/h_2 , which can be solved for m_1 and m_2 . Finally the nondimensional force and moment are found from (26).

The results for the dimensionless contact half-width (\bar{a}) vs. the dimensionless normal force (\bar{F}) for various values of λ are shown in Fig. 3 for $h_1/h_2 = 5$. When Figs. 2 and 3 are compared, it is seen that as h_1/h_2 increases from 1 to 5, the force required to produce a given contact width also increases. This effect is greater for large λ (JKR region, due to elastic deformation) than it is for moderate λ (DMT regime, limited elastic deformation) or small λ (Hertz regime, small adhesion). Figs. 4 shows the dimensionless adhesion half-width difference ($m_1 - m_2$) vs. dimensionless contact half-width (\bar{a}) for different values of λ with $h_1/h_2 = 5$. This measure of the asymmetry of the adhesion zones becomes large for small values of the dimensionless contact radius (\bar{a}). It is also much greater for small λ than for large λ . This result may appear counter-intuitive. However the contact half-width is normalized by a quantity which includes the cube-root of the work of adhesion, whereas λ varies as the two-thirds power of w . Also large λ corresponds to greater elastic deformation which is better capable of accommodating the asymmetry in the work of adhesion. The results for the dimensionless average adhesion length $(m_1 + m_2)/2$ vs. dimensionless contact radius are shown for various values of λ in Fig. 5 for $h_1/h_2 = 5$. Finally the dimensionless moment (\bar{M}) vs. the dimensionless normal force (\bar{F}) are shown for various values of λ in Fig. 6 for $h_1/h_2 = 5$. Note that as the normal force approaches the pull-off force, the moment approaches a finite value, even in the small λ regime where \bar{a} vanishes at pull-off. This result is the combined effect of the asymmetry in the work of adhesion along with the small elastic deformation.

Rolling

The problem of steady state rolling of an elastic cylinder on an elastic half-space (or equivalently one cylinder rolling on another) with Coulomb friction was solved by Carter [14]. According to Carter's solution the leading edge of the contact zone ($d < x < a$) is in a state of stick whereas the trailing edge ($-a < x < d$) is in a state of slip. As in the application to a locomotive wheel [14], the upper body is the driving cylinder. During this rolling motion, the linear velocity of the center of the cylinder is slightly less than ωR , where ω is the angular velocity. The creep velocity represents this velocity difference.

At the nano-scale the shear stress (friction stress) in the slip zone is assumed to be constant, as previously discussed. As with sliding, adhesion affects the relation between the normal force and contact width. The tangential relative displacement (shift) between the bodies is expressed as

$$s(x, t) = u_x^{(2)}(x, 0, t) - u_x^{(1)}(x, 0, t) + C(t), \quad (28)$$

where C represents the rigid body motion of the upper body relative to the lower body. In the stick zone the time derivative of the shift in the moving coordinate system is zero. The stick condition can be written as,

$$\dot{s}(x, t) = V \frac{d}{dx}(u_{x2} - u_{x1}) + \dot{C} = 0, \quad d < x < a \quad (29)$$

where $\dot{C}(t)$ is the constant rigid body slip (or creep) velocity. Furthermore the shear stress is constant in the slip region, i.e.

$$p_x(x) = -\tau_0, \quad -a < x < d \quad (30)$$

The solution of Eq. (2), subject to (29)-(30), can be found by superposition of the solution for a crack external to the stick region and loaded in shear on one side, i.e. the slip zone (Tada et al. [11, p. 107]), the solution of (2) due to the constant creep velocity, and the homogeneous solution of (2). The Mode II stress intensity factors for the external crack problem at the ends of the stick zone are [11]

$$K_{II}(d) = \frac{\tau_0}{\pi^2} \left\{ 2 \sqrt{\frac{a^2 + ad}{a-d}} + \frac{\sqrt{2(a-d)}}{2} \cosh^{-1} \left(\frac{3a+d}{a-d} \right) \right\}$$

$$K_{II}(a) = \frac{\tau_0}{\pi^2} \left\{ 2 \sqrt{\frac{a^2 + ad}{a-d}} - \frac{\sqrt{2(a-d)}}{2} \cosh^{-1} \left(\frac{3a+d}{a-d} \right) \right\} \quad (31)$$

whereas the solution to the creep velocity and the homogeneous solution are

$$p_x(x) = \frac{\dot{C}E}{2V} \sqrt{\frac{a-x}{x-d}} + \frac{D_1}{\sqrt{(a-x)(x-d)}}, \quad d < x < a \quad (32)$$

The requirement that the solution be bounded at $x = a$ and $x = d$ leads to the following equations,

$$D_1 = \frac{\tau_0}{\pi} \left\{ \frac{a-d}{2} \cosh^{-1} \left(\frac{3a+d}{a-d} \right) - \sqrt{2a(a+d)} \right\} \quad (33)$$

$$\frac{\dot{C}}{V} = -\frac{2\tau_0}{\pi E} \cosh^{-1} \left(\frac{3a+d}{a-d} \right). \quad (34)$$

If force equilibrium is written in the x -direction, the applied shear force can be related to the contact width parameter (d) by

$$T = \int_{-a}^a p_x(x) dx = -\tau_0 \sqrt{2a(d+a)} \quad (35)$$

Equation (35) gives the variation of the applied tangential force with the extent of the slip zone. The greater the traction force, the larger is the slip zone. As $d \rightarrow a$ the rolling motion approaches complete slip. Equation (34) gives the dimensionless creep velocity, which is linear in τ_0/E and varies nonlinearly with the slip zone parameter (d/a). As the traction force increases, d increases and hence the magnitude of the creep velocity increases logarithmically according to (34). The meaning of the negative creep velocity is that ωR for the driving wheel is greater than the velocity of the contact zone.

CONCLUSIONS

This paper treats the two-dimensional elastic contact problem of a cylinder on a substrate during a rolling/sliding motion and includes the effect of adhesion using the Baney and Hui version of the Maugis-Dugdale model. During initiation of sliding, there is a central stick zone surrounded by slip regions in the leading and trailing edges. As the tangential force T increases, the lengths of the slip zones increase until complete slip occurs at a certain value of T . During steady sliding the abrasive action of the shear stress can be expected to partially clean the surface, resulting in different leading and trailing edge adhesive properties. This effect is included in the model of steady nano-scale sliding. Variations of the creep velocity and the length of the stick zone with T are determined. As the traction force increases, the stick zone length decreases and the creep velocity increases eventually leading to pure slip with rotation.

REFERENCES

1. O. T. Sari, August 2003, *Master of Science Thesis*, Mechanical Engineering Dept., Northeastern University, Boston, MA.
2. R. S. Bradley, 1932, "The cohesive force between solid surfaces and the surface energy of solids," *Phil. Mag.*, **13**, pp. 853-862.
3. K. L. Johnson, K. Kendall and A. D. Roberts, 1971, "Surface energy and the contact of elastic solids," *Proc. Royal Soc. London Ser. A*, **324**, pp. 3101-3130.
4. B. V. Derjaguin, V. M. Muller and Y. P. Toporov, 1975, "Effect of contact deformations on the adhesion of particles," *J. Coll. and Interface Sci.*, **67**, pp. 314-326.
5. D. Tabor, 1976, "Surface forces and surface interactions," *J. Coll. and Interface Sci.*, **58**, pp. 1-13.
6. J. A. Greenwood, 1997, "Adhesion of Elastic Spheres," *Proc. R. Soc. Lond. A*, **453**, pp. 1277-1297.
7. D. Maugis, 1992, "Adhesion of spheres: the JKR-DMT transition using a Dugdale model," *J. Coll. and Interface Sci.*, **150**, pp. 243-269.
8. J. M. Baney and C.-Y. Hui, 1997, "A Cohesive Zone Model for the Adhesion of Cylinders," *J. Adhesion Sci. and Technology*, **11**, pp. 393-406.
9. J. R. Barber, 2002, *Elasticity*, second edition, Kluwer Academic Publishers.
10. K. L. Johnson, 1985, *Contact Mechanics*, Cambridge University Press.
11. H. Tada, P. C. Paris, and G. R. Irwin, 2000, *The Stress Analysis of Cracks Handbook*, third edition, ASME Press.

12. R. D. Mindlin, 1949, "Compliance of elastic bodies in contact," J. Appl. Mech., **17**, pp. 259-268.
13. A. Erdélyi, *Tables of Integral Transforms*, Bateman Manuscript Project, McGraw-Hill Book Company, New York, (1954).
14. F. W. Carter, 1926, "On the action of a locomotive driving wheel," Proc. Roy. Soc. (London), **A112**, pp. 151-157.

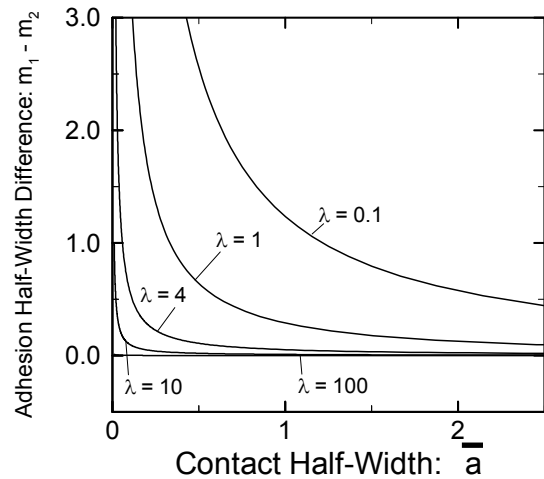


Figure 4. The trailing and leading edge half-width difference ($m_1 - m_2$) vs. contact half-width (\bar{a}) during sliding with $h_1/h_2=2.5$

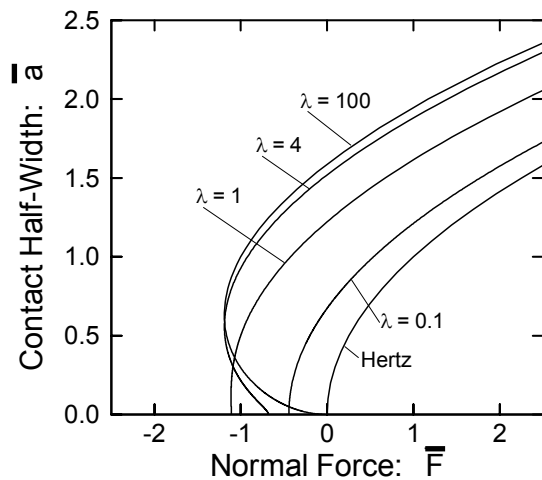


Figure 2. The variation of the dimensionless contact half-width (\bar{a}) with the dimensionless normal load (\bar{F}) for various values of λ .

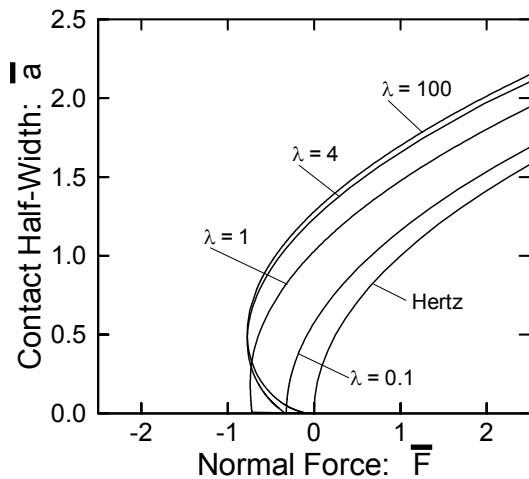


Figure 3. The variation of the dimensionless contact half-width (\bar{a}) with the dimensionless normal load (\bar{F}) for various values of λ during sliding with $h_1/h_2=5$.

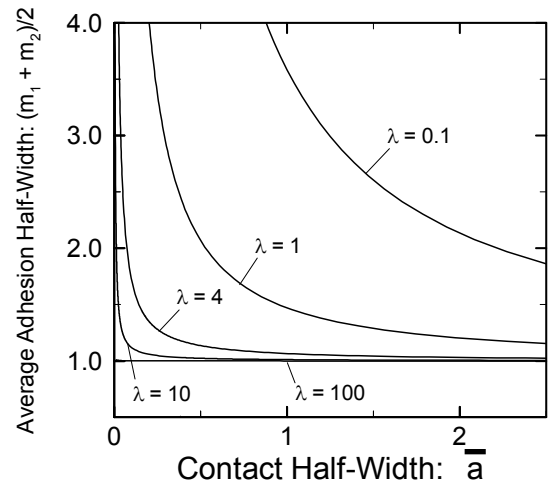


Figure 5. The trailing and leading edge average $(m_1 + m_2)/2$ vs. contact half-width (\bar{a}) during sliding with $h_1/h_2=5$.

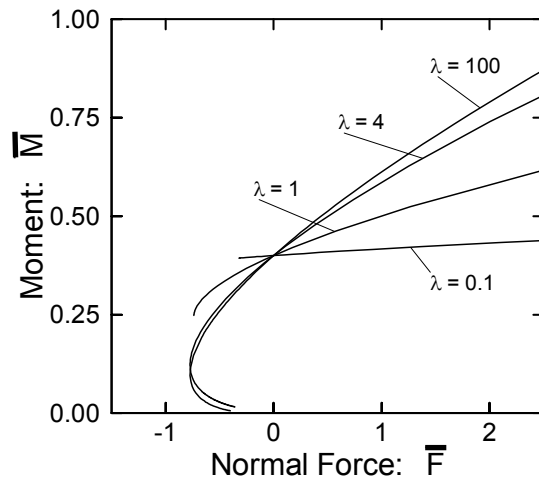


Figure 6. The dimensionless resultant moment (\bar{M}) vs. dimensionless contact half-width (\bar{a}) for various values of λ during sliding with $h_1/h_2=5$.